ARMY RESEARCH LABORATORY

Tensile Creep Strain and Activation Energy

Albert A. Warnas

ARL-TR-455

July 1994

15PO

REPORT DOCUMENTATION PAGE

Form Approved
OMB No. 0704-0188

1. AGENCY USE ONLY *(Leave blank)*	2. REPORT DATE	3. REPORT TYPE AND DATES COVERED
	July 1994	Final Report

4. TITLE AND SUBTITLE
Tensile Creep Strain and Activation Energy in PMMA

5. FUNDING NUMBERS

6. AUTHOR(S)
Albert A. Warnas

7. PERFORMING ORGANIZATION NAME(S) AND ADDRESS(ES)
U.S. Army Research Laboratory
Watertown, MA 02172-0001
ATTN: AMSRL-MA-PA

8. PERFORMING ORGANIZATION REPORT NUMBER
ARL-TR-455

9. SPONSORING/MONITORING AGENCY NAME(S) AND ADDRESS(ES)
U.S. Army Research Laboratory
2800 Powder Mill Road
Adelphi, MD 20783-1197

10. SPONSORING/MONITORING AGENCY REPORT NUMBER

11. SUPPLEMENTARY NOTES

12a. DISTRIBUTION/AVAILABILITY STATEMENT
Approved for public release; distribution unlimited.

12b. DISTRIBUTION CODE

13. ABSTRACT *(Maximum 200 words)*

In a set of PMMA creep curves, at several temperatures under the same dead load, any constant tensile creep strain e will intercept a set of time-temperature points. In PMMA we can relate such a set of time-temperature points to an equivalent set of relaxation time-temperature points associated with a constant activation energy ΔH obtained with the Arrhenius equation. Then ΔH is proportional to e over their common intercepted set of time-temperature points.

14. SUBJECT TERMS
Tensile creep, Activation energy, Arrhenius equation, PMMA

15. NUMBER OF PAGES
14

16. PRICE CODE

17. SECURITY CLASSIFICATION OF REPORT	18. SECURITY CLASSIFICATION OF THIS PAGE	19. SECURITY CLASSIFICATION OF ABSTRACT	20. LIMITATION OF ABSTRACT
Unclassified	Unclassified	Unclassified	UL

NSN 7540-01-280-5500

Standard Form 298 (Rev. 2-89)
Prescribed by ANSI Std Z39-18
298-102

CONTENTS

FIGURES

INTRODUCTION

With dynamic techniques, Read (1) showed a distribution of relaxation times associated with a distribution of activation energies. These distributions were associated with the Arrhenius equation for glassy state temperatures and Read (1) concluded "... that the assumption of a single activation energy which underlies the frequency-temperature superposition principle is invalid in the case of β-relaxation in PMMA.". Likewise McCrum et al. (2) concluded that a constant activation energy ΔH associated with all components of the relaxation time distribution is not unequivocally supportable by time-temperature superposition. The present note indicates that the convergence of two PMMA tensile creep curves represented by two temperatures and the same dead load L_o precludes the use of time-temperature superposition for obtaining activation energies of creep strain. It further associates the total engineering creep strain $e = e(L_o, T, t)$ on a loge-logt plot, with the activation energy $\Delta H = \Delta H(\tau, T)$ through the Arrhenius equation.

$$\log(\tau / \tau_{om}) = \log(t / t_{cf}) = \Delta H / (4.56T) \qquad \text{Equation 1a}$$

where $4.56 = 2.303R$. τ_{om} (in the notation of Read (1)) is associated with "the reciprocal molecular oscillation frequency" as is t_{cf} the time at the convergence point $N_o = N(L_o, e_o, t_{cf})$ of the set of experimental creep curves. Eq. 1a holds if $\tau_{om} = t_{cf}$ (taken in this report as similar to 10^{-13} s as stated in Reference 3) and is "constant for all processes" (1).

References 4 and 5 showed with wave velocity experiments starting at 4 K for a collection of thermoplastics, that a plot of dynamic modulus E versus T has one of two paths depending on the thermoplastic. For semicrystalline plastics there is a temperature T_s-range $4K < T_s < T_{sL}$ where $E = E(T_s)$ has a plateau value in the T_s-range and, when $T > T_{sL}$, $E = E(T)$ decreases rapidly with increasing temperature to the end of the experimental range. The other path is for amorphous plastics where $T_s = T_{sL} = 4$ K so that there is no plateau and $E(T)$ decreases rapidly with T from $E_o(4\text{ K})$. These two paths appear to predict that amorphous plastics are governed by t_{cf} similar to 10^{-13} s and semicrystalline plastics by t_c similar to 10^{-6} s.

The compensation equation takes the form:

$$\log(t / t_c) = (\Delta H / 4.56)(1 / T - 1 / T_M) \qquad \text{Equation 1b}$$

where T_M is the melting temperature and t_c is of the order 10^{-6} s as established with high density polyethylene (HDPE) (6).

We will show that ΔH is proportional to e for PMMA. We found this to be supported by Eq. 1a but not by Eq. 1b.

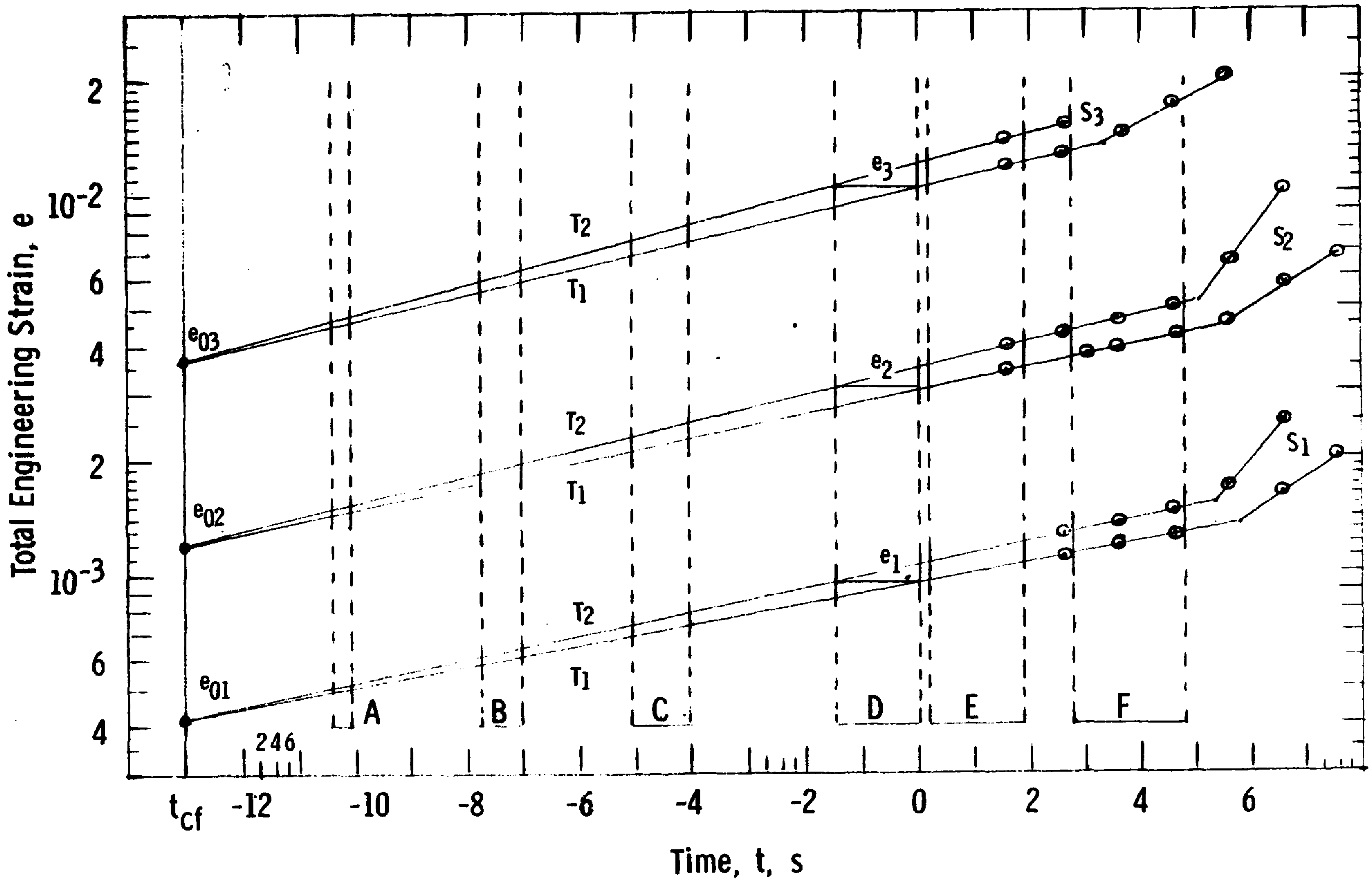

Figure 1. PMMA tensile creep data extrapolated to $N_o = N(S, e_o, t_{cf})$. Stress $S = S(L_o)$ in MPa: $S_1 = 3.55$, $S_2 = 10$, $S_3 = 30$. $T_1 = 293$ K, $T_2 = 333$ K. Elastic strain $e_o = e_o(S) = S / E_o(4\text{ K})$: $e_{o1} = 0.00042$, $e_{o2} = 0.00121$, $e_{o3} = 0.00363$. ΔH in kcal / mol in the t-T intervals: A, 4 kcal / mol; B, 8; C, 12; D, 17.5; E, 20; F, 24. $t_{cf} = 10^{-13}$ s.

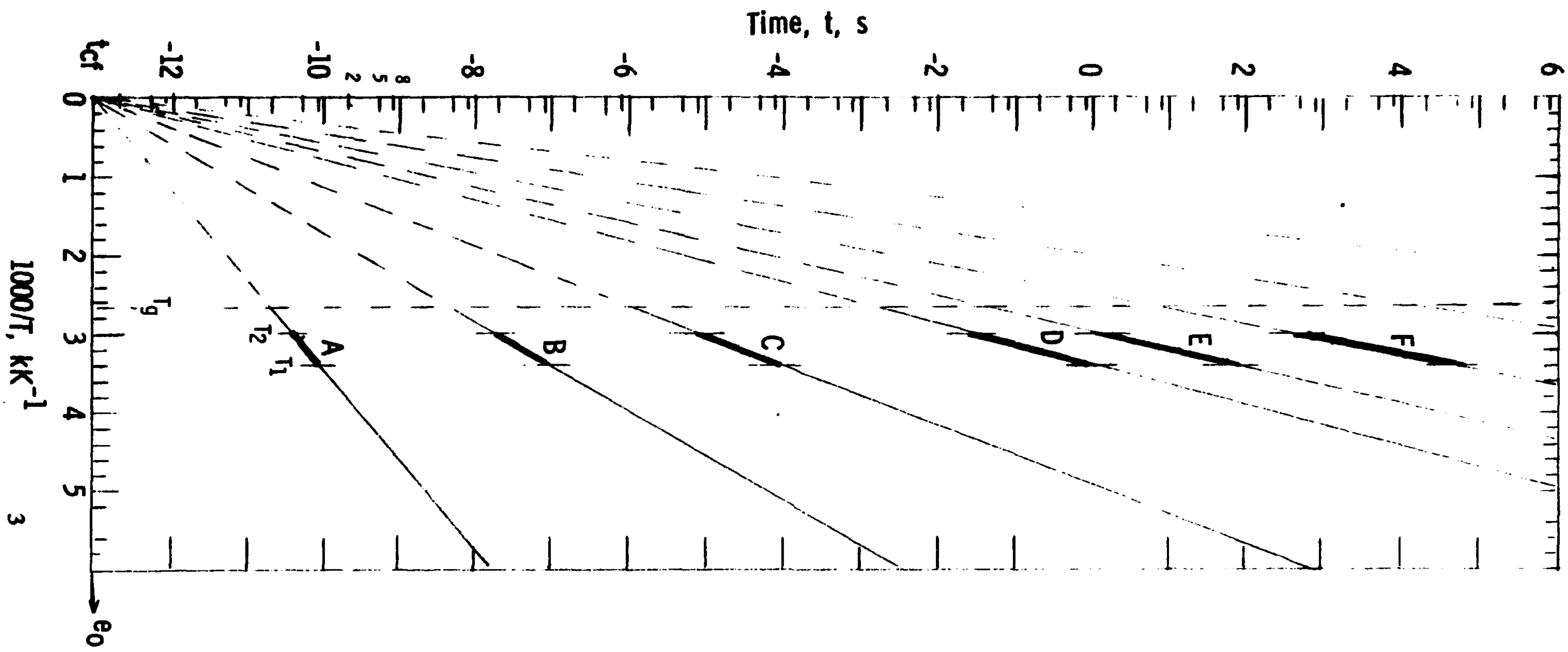

Figure 2. Arrhenius plot with $\log(t / t_{cf}) = \Delta H / (4.56T)$, $t_{cf} = 10^{-13}$ s. Enhanced slope segments are associated with ΔH, in kcal / mol, which are related to the constant strain segments in Fig. 1. The t-T intervals of the enhanced sements are related to the corresponding t-T intervals in Fig. 1. A, 4 kcal /mol; B, 8; C, 12; D, 17.5; E, 20; F, 24; G, 30; H, 40. PMMA glass transition temperature $T_g = 378$ K. $T_1 = 293$ K and $T_2 = 333$ K. Along the 1000 / T axis, where $\Delta H = 0$, $e_o(S)$ is a constant for each $S(L_o)$.

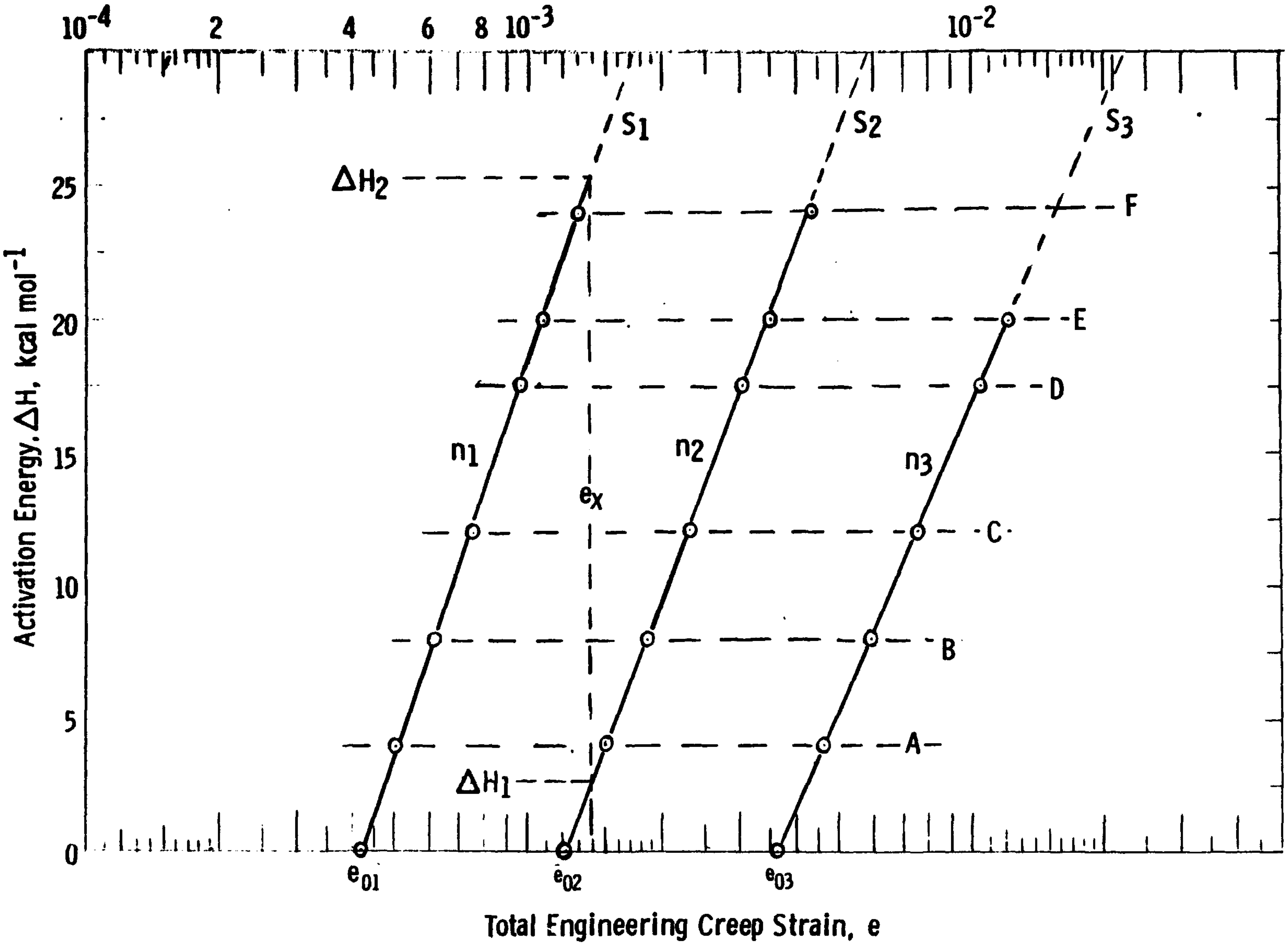

Figure 3. Relation of PMMA tensile creep strain to activation energy from common t-T intervals (in Figs. 1 and 2). $\Delta H = n\log(e / e_o)$. The slope n decreases as $S = S(L_o)$ increases. S in MPa. $S_1 = 3.35$ MPa, $S_2 = 10$, $S_3 = 30$. Each letter, A through H, indicates the set of strains associated with a ΔH. Note that the t-T intervals, where e and ΔH are constant (in Figs. 1 and 2), degenerate to a single point.

DATA and RESULTS

The material is Perspex that is a slightly modified PMMA. Read (1) and McCrum and Morris (7) describe Perspex. In the present note the PMMA tensile creep data is from the literature by Ogorkiewicz (8). However, most of the tensile creep curves reconstructed from this data required interpolation to produce adequate data for this note. In Fig. 1 these tensile creep curves are replotted on a double-log graph and extrapolated to short times to converge at $N_o = N(L_o, e_o, t_{cf})$, independent of temperature, where e_o is the elastic strain due to L_o, independent of temperature. e_o = stress / E_o(4 K), where E_o(4 K) = 8.27 x 10^3 Mpa (1.2 x 10^6 psi) is the dynamic elastic modulus (4) (5). With each L_o, we produced a set of converging creep curves. We may consider each curve (with a distinct constant temperature) of a set, as emanating from the point N_o belonging to the set.

In Fig. 1, a set of tensile creep curves, under constant L_o, with each curve of the set a distinct isotherm, consists of engineering tensile creep strains e associated with t,T points. A selected subset of such t,T points will intercept a constant-strain segment. We subtend each of the selected subsets of t,T points in Fig. 1 by a pair of vertical lines that in turn subtend three individual constant-strain segments. We produced each constant-strain segment under a different L_o. The selected sets of t,T points in Fig. 1 correspond to those in Fig. 2. In Fig. 2, a constant-ΔH segment is proportional to a constant slope that obeys Eq. 1a in which t replaces τ. The enhanced bold-line segments (drawn between vertical lines) consist of sets of t,T points. Each set of t,T points in an enhanced segment has its counterpart in the corresponding selected set of t,T points in Fig. 1. Therefore, in a set of t,T points--subtended between vertical lines in Fig. 1 and selected to correspond to an enhanced line in Fig. 2--the three constant-strain segments are associated with a single constant-ΔH segment. Apparently the activation energy associated with creep strain is dependent on the t, T combination (Eq. 1a) and not on the load producing the strain. That is, ΔH(t,T) is proportional to all e(t, T) in a t,T interval independent of L_o. We show this in Fig. 3. For example, the set of t,T points in the constant-ΔH segment (= 17.5 kcal / mol) between (t_1,T_2) = (3.35 x 10^{-12} s, 333 K) and (t_2,T_1) = (1.25 s, 293 K) in Fig. 2 intercepts the constant-strain segments e_1 = 0.00096, e_2 = 0.00305, and e_3 = 0.0103 produced by L_{o1}, L_{o2}, and L_{o3}, respectively, in Fig. 1. Each of these strains (due to its associated L_o) is proportional to ΔH = 17.5 kcal / mol in Figs. 2 and 3.

From Figs. 1 and 3, in the case of a constant strain common to several adjacent creep curve sets, as L_o decreases ΔH increases and vice versa. This is the source of the statement in Ref. 6 that there is a decrease in ΔH with increasing load (stress). We can easily construct this case in Figs. 1, 2 and 3 when two creep curves from adjacent creep curve sets are in such proximity as to intersect at a common $e_x = e_1(L_{o1}, T_2, t_x) = e_2(L_{o2}, T_1, t_x)$ at the common time t_x, where $L_{o2} > L_{o1}$, $T_2 > T_1$ and $\Delta H_2 > \Delta H_1$ (see Fig. 3).

CONCLUSION

We conclude by means of Fig. 2 and Eq. 1a, that we can associate a constant ΔH with the total engineering creep strain(s) e from Fig. 1. We denote this by:

$$\Delta H(t,T) = {}^{*}n\log[e(L_o, t, T) / e_o(L_o)] \qquad \text{Equation 2}$$

where $^{*}n$ = n(PMMA) = n, in kcal / mol, varies with load in Fig. 3. With Eq. 2, we may obtain the slope $^{*}n$ = n(HDPE) for a set of HDPE tensile creep curves from the data at 9.19 MPa in Ref. 4.

We found no evidence of a "bump"--as that on the PMMA shear creep curve by Lethersich shown in Ref. 9--on any tensile creep curves (before or after reproduction on a double-log graph). (In the elastic and linear viscoelastic range the tensile creep strain is about 1/3 the shear creep strain at sufficiently large times (10).) Otherwise, the Lethersich data---with ΔH = 18 kcal/mol (calculated with $t_{cf} = 10^{-13}$ s in Eq. 1a) at 30°C, 7.3 MPa and an "average relaxation time of 1 s" (9)---agrees with the corresponding ΔH for the present tensile creep data.

Likewise, Read's Fig. 9 (1) relaxation peak value ΔH(peak) = 16.7 kcal / mol (calculated with $t_{cf} = 10^{-14}$ s in Eq. 1a) at t(peak) = 10^{-3} s with 333 K and, at t(peak) = 2.86×10^{-2} s with 294 K, is in near agreement with that of the tensile creep ΔH = 17.5 kcal / mol and the associated t,T points (t = 3.35×10^{-3} s with 333 K and, t = 1.25 s with 293 K). For the associated tensile creep ΔH and t,T points to agree exactly with those associated with the relaxation peaks, we would require a $t_{cf} = 10^{-14}$ s in the adjustment of N_o and the origin in Figs. 1 and 2, respectively.

From Fig. 1, we see that the Boltzmann superposition principle holds between like creep isotherms of sets of isotherms, each set produced by its own L_o. While we found the Boltzmann superposition principle to hold in Fig. 1, we preclude the use of time-temperature superposition on a set of PMMA tensile creep curves below the glass transition temperature. Such a set of creep isotherms at constant L_o shows a natural bent for non-parallelism indicated by their convergence at N_o in Fig. 1. Any correction for parallelism appears to be an approximation for such cases.

Note that Fig. 2 and Eq. 1a holds for amorphous plastics as in PMMA. We expect to find the tensile creep curves of these plastics converging to $N_o = N(e_o, t_{cf})$, where t_{cf} is similar to 10^{-13} s. In that case, we expect polycarbonate (PC), for example, to have an e-ΔH relation qualitatively similar to that for PMMA but quantitatively different according to their dynamic elastic moduli at 4 K (4) (5). We found this to be so when we extrapolated tensile creep curves of PC to short time (unpublished).

For future work, we could use References 4 and 5 as a guide to examine the convergence of the creep curves of some of these thermoplastics at t_c or t_{cf}, and, to examine the ensuing relation of the activation energy to the creep strain.

ACKNOWLEDGMENT

Thanks go to Dr. Bernard M. Halpin, Chief, and Dr. Richard J. Shuford, Group Leader, of MTL, Composites Development Branch, for support of this note during my tenure as emeritus at MTL.

REFERENCES

1 Read, B.E., Polymer 1981, 22, 1581.

2 McCrum, N.G., Pizzoli, M., Chai, C.K., Treuernicht, I., and Hutchinson, J.M., Polymer, 1982, 23, 473.

3 McCrum, N.G., Polymer 1984, 25, 299.

4 Perepechko, I.I. and Golub, P.D., Mekhanika Polimrov (Eng. Trans.), 1973, No 4, July-Aug., 534.

5 Sorokin, V.E. and Perepechko, I.I., Mekhanika Polimorov (Eng. Trans.), 1974, No. 1, Jan.-Feb., 14.

6 Warnas, A.A., Polymer Communications 1991, 32, 83.

7 McCrum, N,G. and Morris, E.L., Proc. Roy. Soc., 1964, A281, 258.

8 Ogorkiewicz, R.M., ed. "Engineering Properties of Thermoplastics", Part III, Chapter 12, Figures 12.1 and 12.6, Wiley, 1970, N.Y.

9 McCrum, N.G., Read, B.E. and Williams, G., "Anelastic and Dielectric Effects in Polymeric Solids", p243, Fig, 8.4, Wiley, 1967, N.Y.

10 Ferry, J.D., "Viscoelastic Properties of Polymers", 3rd Ed., Wiley, 1980, N.Y.

DISTRIBUTION LIST

No. of Copies	To
1	Office of the Under Secretary of Defense for Research and Engineering, The Pentagon, Washington, DC 20301
	Director, U.S. Army Research Laboratory, 2800 Powder Mill Road, Adelphi, MD 20783-1197
1	ATTN: AMSRL-OP-SD-TP, Technical Publishing Branch
1	AMSRL-OP-SD-TA, Records Management
1	AMSRL-OP-SD-TL, Technical Library
	Commander, Defense Technical Information Center, Cameron Station, Building 5, 5010 Duke Street, Alexandria, VA 23304-6145
2	ATTN: DTIC-FDAC
1	MIA/CINDAS, Purdue University, 2595 Yeager Road, West Lafayette, IN 47905
	Commander, Army Research Office, P.O. Box 12211, Research Triangle Park, NC 27709-2211
1	ATTN: Information Processing Office
	Commander, U.S. Army Materiel Command, 5001 Eisenhower Avenue, Alexandria, VA 22333
1	ATTN: AMCSCI
	Commander, U.S. Army Materiel Systems Analysis Activity, Aberdeen Proving Ground, MD 21005
1	ATTN: AMXSY-MP, H. Cohen
	Commander, U.S. Army Missile Command, Redstone Arsenal, AL 35809
1	ATTN: AMSMI-RD-CS-R/Doc
	Commander, U.S. Army Armament, Munitions and Chemical Command, Dover, NJ 07801
1	ATTN: Technical Library
	Commander, U.S. Army Natick Research, Development and Engineering Center Natick, MA 01760-5010
1	ATTN: SATNC-MI, Technical Library
	Commasnder, U.S. Army Satellite Communications Agency, Fort Monmouth, NJ 07703
1	ATTN: Technical Document Center
	Commander, U.S. Army Tank-Automotive Command, Warren, MI 48397-5000
1	ATTN: AMSTA-ZSK
1	AMSTA-TSL, Technical Library
	President, Airborne, Electronics and Special Warfare Board, Fort Bragg, NC 28307
1	ATTN: Library
	Director, U.S. Army Research Laboratory, Weapons Technology, Aberdeen Proving Ground, MD 21005-5066
1	ATTN: AMSRL-WT

No. of Copies	To
	Commander, Dugway Proving Ground, UT 84022
1	ATTN: Technical Library, Technical Information Division
	Commander, U.S. Army Research Laboratory, 2800 Powder Mill Road, Adelphi, MD 20783
1	ATTN: AMSRL-SS
	Director, Benet Weapons Laboratory, LCWSL, USA AMCCOM, Watervliet, NY 12189
1	ATTN: AMSMC-LCB-TL
1	AMSMC-LCB-R
1	AMSMC-LCB-RM
1	AMSMC-LCB-RP
	Commander, U.S. Army Foreign Science and Technology Center, 220 7th Street, N.E., Charlottesville, VA 22901-5396
3	ATTN: AIFRTC, Applied Technologies Branch, Gerald Schlesinger
	Commander, U.S. Army Aeromedical Research Unit, P.O. Box 577, Fort Rucker, AL 36360
1	ATTN: Technical Library
	U.S. Army Aviation Training Library, Fort Rucker, AL 36360
1	ATTN: Building 5906-5907
	Commander, U.S. Army Agency for Aviation Safety, Fort Rucker, AL 3636
1	ATTN: Technical Library
	Commander, Clarke Engineer School Library, 3202 Nebraska Ave., N., Fort Leonard Wood, MO 65473-5000
1	ATTN: Library
	Commander, U.S. Army Engineer Waterways Experiment Station, P.O. Box 631, Vicksburg, MS 39180
1	ATTN: Research Center Library
	Commandant, U.S. Army Quartermaster School, Fort Lee, VA 23801
1	ATTN: Quartermaster School Library
	Naval Research Laboratory, Washington, DC 20375
1	ATTN: Code 6384
	Chief of Naval Research, Arlington, VA 22217
1	ATTN: Code 471
	Commander, U.S. Air Force Wright Research and Development Center, Wright-Patterson Air Force Base, OH 45433-6523
1	ATTN: WRDC/MLLP, M. Forney, Jr.
1	WRDC/MLBC, Mr. Stanley Schulman
	U.S. Department of Commerce, National Institute of Standards and Technology, Gaithersburg, MD 20899
1	ATTN: Stephen M Hsu, Chief, Ceramics Division, Institute for Materials Science and Engineering

No. of Copies	To
1	Committee on Marine Structures, Marine Board, National Research Council, 2101 Constitution Avenue, N.W., Washington, DC 20418
1	Materials Sciences Corporation, Suite 250, 500 Office Center Drive, Fort Washington, PA 19034
1	Charles Stark Draper Laboratory, 555 Technology Square, Cambridge, MA 02139
	Wyman-Gordon Company, Worcester, MA 01601
1	ATTN: Technical Library
	General Dynamics, Convair Aerospace Division, P.O. Box 748, Fort Worth, TX 76101
1	ATTN: Mfg. Engineering Technical Library
	Plastics Technical Evaluation Center, PLASTEC, ARDEC, Bldg. 355N, Picatinny Arsenal, NJ 07806-5000
1	ATTN: Harry Pebly
1	Department of the Army, Aerostructures Directorate, MS-266, U.S. Army Aviation R&T Activity - AVSCOM, Langley Research Center, Hampton, VA 23665-5225
1	NASA - Langley Research Center, Hampton, VA 23665-5255
	U.S. Army Vehicle Propulsion Directorate, NASA Lewis Research Center, 2100 Brookpark Road, Cleveland, OH 44135-3191
1	ATTN: AMSRL-VP
	Director, Defense Intelligence Agency, Washington, DC 20340-6053
1	ATTN: ODT-5A, Mr. Frank Jaeger
	U.S. Army Communications and Electronics Command, Fort Monmouth, NJ 07703
1	ATTN: Technical Library
	U.S. Army Research Laboratory, Electronic Power Sources Directorate, Fort Monmouth, NJ 07703
1	ATTN: Technical Library
	Director, U.S. Army Research Laboratory, Watertown, MA 02172-0001
2	ATTN: AMSRL-OP-WT-IS, Technical Library
5	Author